EUROPEAN ORGANIZATION FOR NUCLEAR RESEARCH

Proposal to the ISOLDE and Neutron Time-of-Flight Committee

CERN-INTC-2016-057 / INTC-P-486
07/10/2016

Collinear laser spectroscopy on chromium: from $N = Z$ towards $N = 40$

October 7, 2016

H. Heylen[1], B. Cheal[2], M.L. Bissell[3], K. Blaum[1], R.F. Garcia Ruiz[3], W. Gins[4], C. Gorges[5], S. Kaufmann[5], M. Kowalska[6], J. Krämer[5], S. Malbrunot-Ettenauer[6], G. Neyens[4], R. Neugart[1,7], L. Vázquez[8], W. Nörtershäuser[5], R. Sánchez[9], C. Wraith[2], L. Xie[3], Z.Y. Xu[4], X.F. Yang[4], D.T. Yordanov[8]

[1] *Max-Planck-Institut für Kernphysik, D-69117 Heidelberg, Germany*

[2] *Oliver Lodge Laboratory, Oxford Street, University of Liverpool, L69 7ZE, United Kingdom*

[3] *The University of Manchester, Manchester M13 9PL, United Kingdom*

[4] *KU Leuven, Instituut voor Kern- en Stralingsfysica, 3001 Leuven, Belgium*

[5] *Institut für Kernphysik, TU Darmstadt, D-64289 Darmstadt, Germany*

[6] *ISOLDE, Experimental Physics Department, CERN, CH-1211 Geneva 23, Switzerland*

[7] *Institut für Kernchemie, Universität Mainz, D-55128 Mainz, Germany*

[8] *Institut de Physique Nucléaire, CNRS-IN2P3, Université Paris-Sud, Paris-Saclay, 91406 Orsay, France*

[9] *GSI Helmholtzzentrum für Schwerionenforschung, D-64291 Darmstadt, Germany*

Spokespersons: Bradley Cheal (Bradley.Cheal@liverpool.ac.uk), Hanne Heylen (hanne.heylen@cern.ch)

Contact person: Hanne Heylen (hanne.heylen@cern.ch)

Abstract: The aim of this proposal is to determine the nuclear spins, magnetic dipole moments, electric quadrupole moments and changes in mean-square charge radii of $^{48-61}$Cr ($Z = 24$) using collinear laser spectroscopy at the COLLAPS beam line. These measurements will enable the study of the evolution of collectivity and the wave function configuration along the Cr isotopic chain. The isotopes between $N = 24$ and $N = 37$ exhibit a rich variety in nuclear structure, including deformation near $N = Z = 24$, the $N = 28$ shell closure, the suggested appearance of a new magic number at $N = 32$ and the development of collectivity towards $N = 40$. With the improvements in Cr yields achieved by the development of a laser ionisation scheme and demonstrated in a recent mass measurement experiment at ISOLTRAP, measurements from $N = Z$ up to $N = 37$ should be feasible.

Requested shifts: 14 shifts of radioactive beam in one run

1 Introduction

High-resolution collinear laser spectroscopy has proven to be an invaluable tool to study the nuclear structure of exotic nuclei [1]. From the measured hyperfine spectra, nuclear spins, moments and changes in mean-square charge radii can be extracted which allow the investigation of single-particle as well as collective effects in the wave function and how these evolve along the isotopic chain.
At the collinear laser spectroscopy beam line COLLAPS at ISOLDE, several experiments have been performed at and around the $Z = 20$ and $Z = 28$ magic numbers, highlighting the rich structural diversity in this region (see for example [2–6]). In between $Z = 20$ and $Z = 28$ however, the experimental information on moments and charge radii remains limited. A notable exception is the Mn ($Z = 25$) isotopic chain, for which the ground- and isomeric state properties were recently studied in collinear laser spectroscopy experiments at JYFL and ISOLDE [7–11]. These revealed a rapidly changing nuclear structure between $N = 25$ and $N = 39$, calling for a more detailed investigation in the neighbouring isotopic chains. Here, were propose to measure the spins, magnetic moments, quadrupole moments and changes in mean-square charge radii of Cr ($Z = 24$) at COLLAPS in ISOLDE. With an exactly half-filled $\pi f_{7/2}$ proton orbital, many structural effects are expected to be even more pronounced in Cr than in Mn.

2 Physics motivation

Nuclear shell structure is known to vary drastically when going to exotic regions of the nuclear chart, giving rise to interesting phenomena such as rapid level migrations, new magic numbers and islands of inversion. In the region around Ca ($Z = 20$) and Ni ($Z = 28$), several such effects have been observed.

The possibility of a new magic number at $N = 32$ was first discussed based on the elevated $E(2_1^+)$-values and reduced $B(E2)$-values in $^{52}_{20}\text{Ca}_{32}$, $^{54}_{22}\text{Ti}_{32}$ and $^{56}_{24}\text{Cr}_{32}$ [12–16]. Also the two-neutron separation energies point to an increased stability at $N = 32$ [17, 18], associated with a substantial subshell gap between the $\nu p_{3/2}$ and $\nu f_{5/2}$ orbitals. This $N = 32$ subshell gap arises due to the monopole part of the tensor component which shifts the $\nu f_{5/2}$ neutron orbital up when protons are removed from the $\pi f_{7/2}$ orbital [19]. As such, the subshell gap is expected to be largest for a completely empty $\pi f_{7/2}$ orbital at $Z = 20$ and to become weaker with increasing Z. Indeed, Cr is the isotopic chain with the highest Z for which the systematics of the even-even nuclei (see left side of Fig. 1) show evidence for the suggested $N = 32$ magicity.
The recent measurement of the Ca ($Z = 20$) moments and mean-square charge radii up to $N = 32$ have however raised some important questions about the magic nature of $N = 32$ [5, 20]. The experimental determination of the magnetic moments has demonstrated that cross shell neutron excitations across $N = 32$ are essential for a correct theoretical reproduction of $^{49,51}\text{Ca}_{29,31}$. Nevertheless, no strong conclusion on the strength of $N = 32$ shell closure can be made since the neutron excitations are of the $M1$-type (between the $\nu p_{3/2}$ and $\nu p_{1/2}$ spin-orbit partners) which are known to strongly influence magnetic

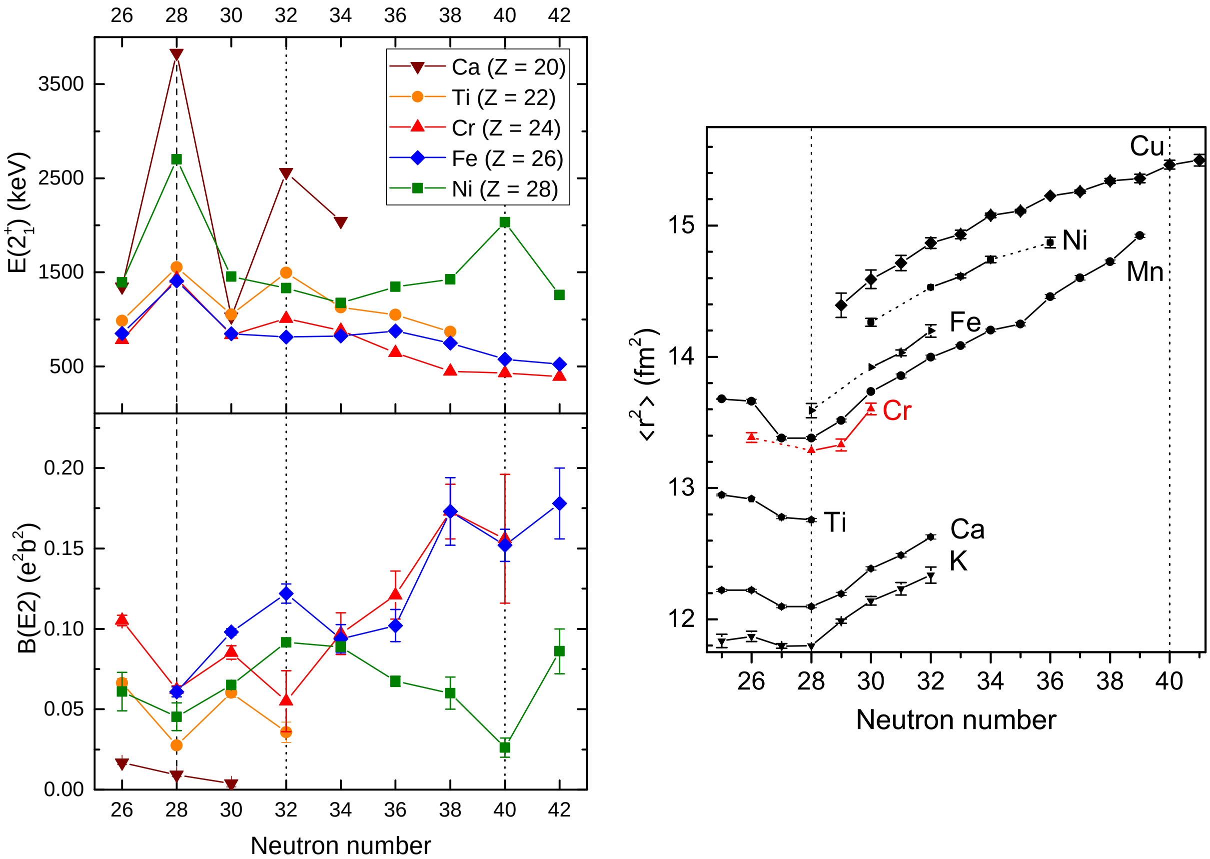

Figure 1: Left: Energies of the first excited 2^+ states (top) and $E2$ transition probabilities (bottom) of the even-even nuclei between Ca and Ni, data taken from [21]. Right: Experimentally known mean-square charge radii from K to Cu, figure adapted from [11].

moments, even on the level a few percent of admixture. More curious are the mean-square charge radii results. Whereas across the chart of nuclides, shell closures manifest themselves as local minima in the mean-square charge radii trend, in the Ca isotopes an increase in charge radii towards $N = 32$ is observed, at variance with the expected behaviour if $N = 32$ were a good shell closure. Measurements of the Cr mean-square charge radii and nuclear moments up to, and beyond $N = 32$, are therefore necessary to better understand these intriguing results.

More neutron-rich, the region below $^{68}_{28}\mathrm{Ni}_{40}$ has recently received a considerable amount of attention. In the proton-magic Ni ($Z = 28$) isotopes, the high $E(2^+_1)$ and low $B(E2)$-values in $^{68}\mathrm{Ni}_{40}$ are indications for a (sub)shell closure at $N = 40$ [22–24]. However, the rather smooth trend in two-neutron separation energies at $N = 40$ suggests that the subshell gap is not well pronounced and localized at $Z = 28$ [25]. For nuclei below $Z = 28$, the weak $N = 40$ subshell gap is not sufficiently strong to stabilise the nuclei in a spherical shape and a strong increase in deformation is observed, as can be inferred from the systematics of the Fe ($Z = 24$) and Cr ($Z = 26$) isotopes in the left part of

Fig. 1. This deformation is explained in terms of np-nh excitations across the $N = 40$ and $Z = 28$ (sub)shell gaps which strongly enhance the quadrupole correlations due to the presence of the (quasi/pseudo-SU(3)) quadrupole partners near the Fermi level [26].
In the beginning of 2016, the development of ground state collectivity in Cr was studied via high-precision mass measurements at ISOLTRAP [27, 28]. Although the results are still preliminary, the two-neutron separation energies are found to be gradually curving upwards. Contrary to the AME2012 two-neutron separation energies [29] which abruptly change between $N = 36$ and $N = 38$, these new results suggest a more gradual onset of deformation. However, as illustrated for Mn ($Z = 25$), such gradual changes in two-neutron separation energies can be accompanied by a sudden increase in mean-square charge radii [11]. As shown in the right part of Fig. 1, from $N = 35$ onwards, a rapid increase in Mn mean-square charge radii is observed. This suggests a strong increase in deformation, in good agreement with the previously determined magnetic and quadrupole moments [8–10]. A measurement of the mean-square charge radii in the neighbouring Cr isotopic chain would provide complementary information on the onset of collectivity and would, in particular, enable the investigation of its dependence on Z. As the half-filled $\pi f_{7/2}$ orbital in Cr boosts the quadrupole collectivity, it will be interesting to see whether the increase in mean-square charge radii happens already earlier in Cr than in Mn.

At the other side of the valley of stability, the isotopes around $N = Z = 24$ are found to be strongly deformed. Since the protons and neutrons in these isotopes occupy the same, half-filled, $f_{7/2}$ orbital, they coherently contribute to the development of prolate deformation. With 24 protons and 24 neutrons, ^{48}Cr has the maximum number of valence particles and can be well described as a rigid rotor [30]. The collective behaviour is nevertheless quickly reduced when neutrons are added to the $\nu f_{7/2}$ orbital and shell effects become important towards $N = 28$. Hence, also closer to stability, the nuclear properties vary significantly over the range of only a few neutron numbers.

In order to explore the rich structural evolution in the Cr isotopes described above, we aim to measure the mean-square charge radii, spins and nuclear moments of $^{48-61}$Cr$_{24-37}$ using high-resolution collinear laser spectroscopy.
The mean-square charge radius is an excellent observables to study the size and shape of a nucleus and hence to probe the deformation along the isotopic chain. To date, however, only the mean-square charge radii of the stable $^{50,52-54}$Cr isotopes have been studied. Radii have the important advantage that they can be measured for, and directly compared between even-even, odd-A and odd-odd isotopes, not restricted to non-zero spin values. Measurements of the radii of radioactive Cr will therefore not only give information on structural changes along the Cr isotopes, but will provide a benchmark for future measurements in the region. As illustrated in the right part of Fig. 1, below $Z = 28$, Mn is the only case for which the a long sequence of charge radii extends beyond $N = 32$, towards $N = 40$. Note that the calibration of the mass and field shift factors needed to relate the measured isotope shifts with the mean-square charge radii is relatively straightforward, since Cr has four naturally occurring isotopes for which the charge radii are measured via non-optical techniques [31].
For the odd-neutron Cr isotopes, complementary insights in the nuclear structure can be

Table 1: Overview of the experimentally known spins, magnetic moments and quadrupole moments of the odd-neutron Cr isotopes [32].

	N	I^{π}	μ (μ_N)	Q_s (b)
^{49}Cr	25	$5/2^-$	0.476(3)	-
^{51}Cr	27	$7/2^-$	$(-)0.934(5)$	-
^{53}Cr	29	$3/2^-$	$-0.47454(3)$	$-0.15(5)$
^{55}Cr	31	$3/2^-$	-	-
^{57}Cr	33	$(3/2)^-$	-	-
^{59}Cr	35	$(1/2)^-$	-	-
^{61}Cr	37	$(5/2)^-$	-	-

obtained via measurements of the magnetic moments and quadrupole moments. The rapid change in nuclear structure in exotic nuclei poses serious challenges for state-of-the-art shell model calculations which have to correctly take into account the subtle competition between single-particle and collective degrees of freedom. Since the magnetic moment and quadrupole moments are sensitive to the wave function composition and quadrupole collectivity, respectively, they provide necessary information to test and improve the currently available models. Nevertheless, so far no moments are known beyond $N = 29$, as shown in Table 1.

Furthermore, also the nuclear spins of the most neutron-rich odd-A Cr isotopes are only tentatively assigned. These assignments are usually based on indirect techniques such as β-decay or even regional systematics, which sometimes result in the wrong conclusions (see for example reference [3]). Measurements of hyperfine spectra, on the other hand, allow the direct and unambiguous determination of nuclear spins and are hence indispensable to construct reliable level schemes.

3 Experiment

To extract spins, magnetic moments, quadrupole moments and changes in mean-square charge radii, we propose to measure the hyperfine spectra of $^{48-61}$Cr using the well-established bunched beam, fluorescence detected collinear laser spectroscopy technique at the COLLAPS beam line. A detailed description of the set-up and technique can for example found in references [4, 33].

The Cr beam will be produced by the bombardment of 1.4-GeV protons on a UC_x target, selectively ionised in the resonance ionisation laser ion source (RILIS), mass separated in the HRS and bunched in the ISCOOL cooler-buncher. Our measurements will greatly benefit from the significant enhancement in Cr yields as a result of the recent development of a laser ionisation scheme [34].

To perform laser spectroscopy in the chromium atom, the ionic beam will be neutralised in a Na-vapour filled charge exchange cell. Several strong atomic transitions are known, although not all of them are suitable to extract nuclear information because of their

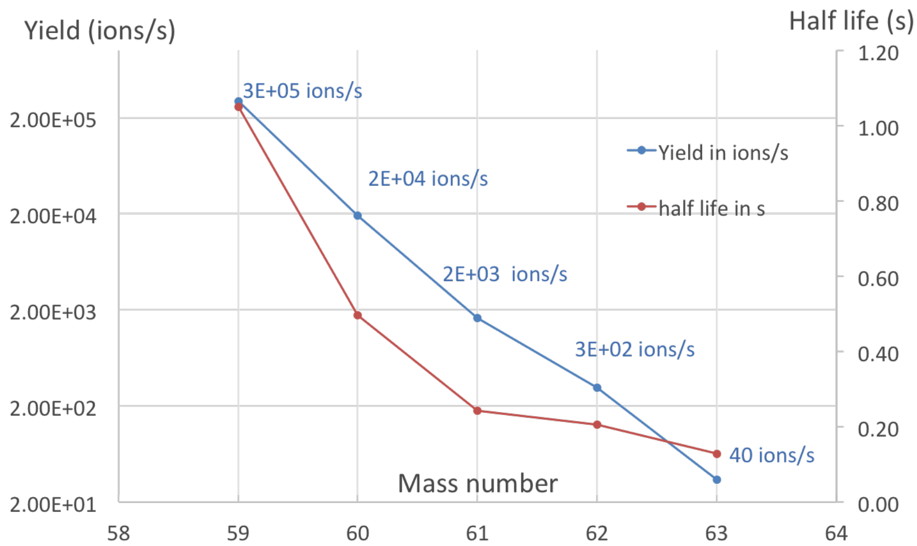

Figure 2: Experimentally observed yields during the 2016 Cr run of ISOLTRAP [28].

collapsed hyperfine structure. In that respect, the 520 nm transition from the $3d^5 4s\ ^7S_2$ metastable state at 7593.16 cm^{-1} to the $3d^5 4p\ ^5P_1$ state at 26801.93 cm^{-1} seems promising due to its relatively large hyperfine splitting, in combination with a sizeable field shift associated with $s-p$ transitions. In addition to this, a few other potentially suitable transitions exists for which the hyperfine parameters are unknown. Therefore, we request a separate stable beam test before the experiment to determine the most efficient and optimal transition.

4 Beam time request

In Fig. 2, the experimentally observed yields of the neutron-rich Cr isotopes are shown along with the half-lives [28]. For ^{48,49}Cr, the yields are conservatively estimated to be $1.2 \cdot 10^4$ ions/μC and $2.2 \cdot 10^4$ ions/μC based on the measured release curve of ^{59}Cr and Fluka calculations [35]. Bunched-beam, fluorescence detected collinear laser spectroscopy is therefore feasible from ^{48}Cr up to ^{61}Cr.

We request 3 shifts of stable beam to setup and optimise the experimental apparatus. This time will additionally be used to measure several hyperfine spectra of each of the four stable Cr isotopes (^{50,52,53,54}Cr) for the calibration of the mass and field shift factors and the nuclear moments. Throughout the run, ^{52}Cr will be used as a reference for the isotope shift measurements while ^{53}Cr will provide the reference for the hyperfine A and B parameters of the odd-even Cr isotopes.
From experience in previous experiments using transitions with similar strengths and realistically assuming a 10% population of the atomic state of interest in the charge exchange process, the measurements will require 14 shifts of radioactive Cr beam. The total beam request is detailed in Table 2.
For the well-produced isotopes with yields larger than 10^5 ions/s, we request 1 shift

Table 2: Summary of the beam request. All beams are produced using an UC_x target + RILIS combination, mass separated in the HRS and bunched in ISCOOL. The yields are quoted assuming a proton beam current of 2 μA.

	Yield (UC_x + RILIS)	Number of shifts
$^{55-59}$Cr	$> 10^5$ ions/s	5
^{48,49,60}Cr	$\sim 2 \cdot 10^4$ ions/s	6
^{61}Cr	$2 \cdot 10^3$ ions/s	3
$^{50,52-54}$Cr	stable	3
^{52,53}Cr	stable	4
	Total: 14	
	+ 3 shifts of stable beam just before the experiment	
	+ 4 shifts of stable beam on a separate occasion to verify the transition	

per isotope. This estimate includes at least three independently measured spectra per isotope, each individual spectrum calibrated against a reference scan. Note that the required time doesn't scale with production yields because a) the detection rate of the PMTs is limited to 10^7 photons/s and b) a large part of the total time is dedicated to the frequent mass changes necessary for the reference scans. More time will be needed for the less produced isotopes and hence we request 6 shifts in total for ^{48,49,60}Cr and 3 shifts for ^{61}Cr. This measurement of this last isotope is challenging due to the low production yield in combination with the fact that it has a non-zero spin, and hence a larger range need to be scanned to measure all peaks in the hyperfine spectrum.

Summary of requested shifts: 14 shifts of radioactive beam are being requested for the study of $^{48-61}$Cr (as summarised in Table 2).

References

[1] P. Campbell, I. D. Moore, and M. R. Pearson. In: *Prog. Part. Nucl. Phys.* 86 (2016), pp. 127 –180.

[2] K. T. Flanagan et al. In: *Phys. Rev. Lett.* 103 (14 2009), p. 142501.

[3] B. Cheal et al. In: *Phys. Rev. Lett.* 104 (25 2010), p. 252502.

[4] J. Papuga et al. In: *Phys. Rev. Lett.* 110 (17 2013), p. 172503.

[5] R. F. Garcia Ruiz et al. In: *Nature Physics* 12 (2016), pp. 594–598.

[6] X. F. Yang et al. In: *Phys. Rev. Lett.* 116 (18 2016), p. 182502.

[7] F. C. Charlwood et al. In: *Phys. Lett. B* 690.4 (2010), pp. 346 –351.

[8] C. Babcock et al. In: *Phys. Lett. B* 750 (2015), pp. 176 –180.

[9] H. Heylen et al. In: *Phys. Rev. C* 92 (4 2015), p. 044311.

[10] C. Babcock et al. In: *Physics Letters B* 760 (2016), pp. 387 –392.

[11] H. Heylen, C. Babcock, et al. In: *Submitted to PRC* arXiv:1609.05021 (2016).
[12] A. Huck et al. In: *Phys. Rev. C* 31 (6 1985), pp. 2226–2237.
[13] J.I. Prisciandaro et al. In: *Physics Letters B* 510.14 (2001), pp. 17 –23.
[14] R.V.F Janssens et al. In: *Phys. Lett. B* 546.12 (2002), pp. 55 –62.
[15] D.-C. Dinca et al. In: *Phys. Rev. C* 71 (4 2005), p. 041302.
[16] A. Bürger et al. In: *Physics Letters B* 622.12 (2005), pp. 29 –34.
[17] C. Guénaut et al. In: *J. Phys. G* 31.10 (2005), S1765.
[18] F. Wienholtz et al. In: *Nature* 498.7454 (2013), pp. 346–349.
[19] T. Otsuka et al. In: *Phys. Rev. Lett.* 95 (23 2005), p. 232502.
[20] R. F. Garcia Ruiz et al. In: *Phys. Rev. C* 91 (4 2015), p. 041304.
[21] B. Pritychenko et al. In: *At. Data Nucl. Data Tables* 107 (2016), pp. 1 –139.
[22] M. Bernas et al. In: *Phys. Lett. B* 113.4 (1982), pp. 279 –282.
[23] R. Broda et al. In: *Phys. Rev. Lett.* 74 (6 1995), pp. 868–871.
[24] O. Sorlin et al. In: *Phys. Rev. Lett.* 88 (9 2002), p. 092501.
[25] C. Guénaut et al. In: *Phys. Rev. C* 75 (4 2007), p. 044303.
[26] S. M. Lenzi et al. In: *Phys. Rev. C* 82 (5 2010), p. 054301.
[27] S. Kreim, V. Manea, et al. Addendum to the ISOLDE and Neutron Time-of-Flight Committee. (2016).
[28] ISOLTRAP. private communication. (2016).
[29] M. Wang et al. In: *Chin. Phys. C* 36.12 (2012), p. 1603.
[30] F. Brandolini et al. In: *Nuclear Physics A* 642.3 (1998), pp. 387 –406.
[31] H. D. Wohlfahrt et al. In: *Phys. Rev. C* 23 (1 1981), pp. 533–548.
[32] Stone N. J. Report No. INDC(NDS)-0658, Nuclear Data Section of the IAEA, Vienna. (2014).
[33] B. Cheal and K. T. Flanagan. In: *J. Phys. G* 37.11 (2010), p. 113101.
[34] T. Day Goodacre et al. In: *arXiv:1512.07875* (2015).
[35] T. Stora. private communication. (2016).

Appendix

DESCRIPTION OF THE PROPOSED EXPERIMENT

The experimental setup comprises: COLLAPS

Part of the	Availability	Design and manufacturing
COLLAPS	☒ Existing	☒ To be used without any modification

HAZARDS GENERATED BY THE EXPERIMENT:
Hazards named in the document relevant for COLLAPS

Additional hazards: None